

# The Effects of Optogenetic Activation of Astrocytes on Spike-and-Wave Discharges in Genetic Absence Epileptic Rats

Annals of Neurosciences

29(1) 53–61, 2022

© The Author(s) 2022

Reprints and permissions:

in.sagepub.com/journals-permissions-india

DOI: 10.1177/09727531211072423

journals.sagepub.com/home/aon



Merve Özgür<sup>1,2,3</sup> , Mustafa Görkem Özyurt<sup>4,5</sup>,  
Sertan Arkan<sup>6</sup> and Safiye Cavdar<sup>3</sup>

## Abstract

**Background:** Absence seizures (petit mal seizures) are characterized by a brief loss of consciousness without loss of postural tone. The disease is diagnosed by an electroencephalogram (EEG) showing spike–wave discharges (SWD) caused by hypersynchronous thalamocortical (TC) oscillations. There has been an explosion of research highlighting the role of astrocytes in supporting and modulating neuronal activity. Despite established *in vitro* evidence, astrocytes' influence on the TC network remains to be elucidated *in vivo* in the absence epilepsy (AE).

**Purpose:** In this study, we investigated the role of astrocytes in the generation and modulation of SWDs. We hypothesize that disturbances in astrocytes' function may affect the pathomechanism of AE.

**Methods:** To direct the expression of channelrhodopsin-2 (ChR2) rAAV8-GFAP-ChR2(H134R)-EYFP or to control the effect of surgical intervention, AAV-CaMKIIa-EYFP was injected into the ventrobasal nucleus (VB) of the thalamus of 18 animals. After four weeks following the injection, rats were stimulated using blue light (~473 nm) and, simultaneously, the electrophysiological activity of the frontal cortical neurons was recorded for three consecutive days. The animals were then perfused, and the brain tissue was analyzed by confocal microscopy.

**Results:** A significant increase in the duration of SWD without affecting the number of SWD in genetic absence epileptic rats from Strasbourg (GAERS) compared to control injections was observed. The duration of the SWD was increased from  $12.50 \pm 4.41$  s to  $17.44 \pm 6.07$  following optogenetic stimulation in GAERS. The excitation of the astrocytes in Wistar Albino Glaxo Rijswijk (WAG-Rij) did not change the duration of SWD; however, stimulation resulted in a significant increase in the number of SWD from  $18.52 \pm 11.46$  bursts/30 min to  $30.17 \pm 18.43$  bursts/30 min. Whereas in control injection, the duration and the number of SWDs were similar at pre- and poststimulus. Both the background and poststimulus average firing rates of the SWD in WAG-Rij were significantly higher than the firing recorded in GAERS.

**Conclusion:** These findings suggest that VB astrocytes play a role in modulating the SWD generation in both rat models with distinct mechanisms and can present an essential target for the possible therapeutic approach for AE.

## Keywords

Optogenetics, Spike-and-wave discharges, Typical absence epilepsy, GAERS, WAG-Rij

Received 23 September 2021; accepted 29 November 2021

## Introduction

Astrocytes are specialized glial cells that contribute to various functions in the brain, including synaptic (a canonical astrocytic feature of glutamate uptake and recycling), neuronal, network, and cognitive processes.<sup>1–3</sup> Accumulating evidence has shown that astrocytes play an essential role in the active control of neuronal activity.<sup>4–8</sup> It has been shown *in situ* that astrocytes in the ventrobasal nucleus (VB) of the thalamus behave as independent glutamate suppliers. Astrocytes lead to long-lasting N-methyl-D-aspartic acid (NMDA)-mediated activation of thalamocortical (TC) neurons both spontaneously and in response to mGluR activation.<sup>9</sup> VB astrocytes can respond to synaptic stimulation

<sup>1</sup> Graduate School of Health Sciences, Division of Neuroscience, Koc University, Istanbul Turkey

<sup>2</sup> Department of Anatomy, Faculty of Medicine, Izmir University of Economics, Izmir, Turkey

<sup>3</sup> Department of Anatomy, Koç University School of Medicine, Istanbul, Turkey

<sup>4</sup> Graduate School of Sciences and Engineering, Koç University, Istanbul, Turkey

<sup>5</sup> Queen Square Institute of Neurology, University College London, London, United Kingdom

<sup>6</sup> Department of Experimental Medical Science, Molecular Neurobiology Unit, Lund University, Lund, Sweden

### Corresponding author:

Merve Özgür, School of Health Sciences, Koç University, Sariyer, Istanbul 34450, Turkey.

E-mail: merve.oezguererat@med.uni-goettingen.de



and interact with neighboring neurons,<sup>10</sup> and this organization might play a functional role in processing somatosensory information<sup>11,12</sup> and modulation of TC network activities.<sup>13</sup> Furthermore, the thalamic glial cells' response to synaptic afferents differs from that of TC neurons. Therefore, these cells are likely to form a distinct cellular and synaptic integration level within the VB thalamus.<sup>13</sup>

Absence epilepsy (AE) is a neurological disease characterized by concomitant periodic generalized spike-and-wave discharges (SWD; 3–5 Hz in humans, 5–9 Hz in animals) in the electroencephalogram (EEG) with an alteration of consciousness and behavioral arrest.<sup>14</sup> Several researchers have reported dysfunctional corticothalamocortical circuitry in AE<sup>15–19</sup> with the notion that for the occurrence of SWD, both properly functioning and structurally normal thalamus and cortex are essential.<sup>20–22</sup> Absence seizures result from an imbalance in glutamate and gamma-aminobutyric acid (GABA) neurotransmission.<sup>23</sup> Several studies have postulated that astrocytes contribute to the pathogenesis of AE.<sup>24–26</sup> Specifically, the calcium-dependent release of glutamate from astrocytes has attracted particular interest.<sup>27–29</sup> It may exaggerate epileptic activity by an excitatory feedback loop or trigger epileptic activity through NMDA receptors.<sup>25,30–32</sup> Whether the epileptiform activity is a direct cause of astrocytic glutamate release has been a matter of debate,<sup>23,30</sup> and the exact signaling pathway is yet to be discovered.

Wistar Albino Glaxo rats from Rijswijk (WAG-Rij) and Genetic Absence Epileptic Rats from Strasbourg (GAERS) are two well-validated genetic rat models with typical AE. These models represent most of the genetic and behavioral disturbances observed in human patients with typical AE.<sup>33,34</sup> The role of astrocytes in the VB nucleus of the thalamus in the AE has not yet been acknowledged. The major aim of our study is to investigate the role of the direct activation of thalamic astrocytes in the AE animal models and compare the two most used animal models of AE. To understand this, we stimulated the astrocytes in the VB thalamus by using optogenetics, simultaneously recorded the electrophysiological activity of frontal cortical neurons, and compared the results between GAERS and WAG-Rij rats.

## Methods

### Animals

In the present study, a total of 18 male animals (aged three to six months) were used—nine from each strain (GAERS and WAG-Rij).<sup>15,16</sup> Rats were randomly and individually assigned to control and experiment groups. Four animals from each strain were used for GFAP-AAV optogenetic manipulation. To avoid the confounding effects, such as differences arising from day-to-day variation and hour-to-hour variation, optogenetic experiments were repeated on three different days and at different hours.<sup>35</sup> Before starting the optogenetic manipulation, one animal from each strain was used for

confirming the viral expression. For photostimulation of astrocytes, the rats received a unilateral infusion of the virus, containing the GFAP promoter in ChR2: AAV8-GFAP-ChR2(H134R)-EYFP (provided by Dr Karl Deisseroth; UNC Vector Core, NC, USA) into the VB of the thalamus. Control rats received the AAV5-CaMKIIa-EYFP virus (UNC Vector Core), which expresses the receptor without ChR2. The animals were kept at the Koç University vivarium and were housed individually on a 12-h light/dark cycle with food and water *ad libitum* in an environment at 23 ± 1°C. The rats were acclimatized to the laboratory for seven days prior to the start of the procedure.

### Surgery

Rats weighing 250 g to 400 g were anesthetized initially with 5% isoflurane (vol/vol) and maintained between 2 to 3% throughout the surgery (Harvard Apparatus, USA). The head of the animal was placed in a stereotaxic frame (Stoelting, Model 51600, Wood Dale, IL, USA). Bregma was taken as the reference point, and coordinates for the ventrobasal thalamus were calculated according to the Rat Brain Atlas of Paxinos and Watson<sup>36</sup> (AP: –3.6 mm, for ML: –3 mm, and for DV: –6.4 mm). The scalp was sutured, and the rats received a subcutaneous injection of 5 g/g Carprofen (Pfizer) for prolonged pain relief. A Hamilton syringe (26 ga) was lowered into the VB thalamus, and 0.5 µL of virus ( $3 \times 10^{12}$  virus molecules/mL) was injected at a flow rate of 0.1 µL/min. Afterward, high-impedance bipolar multiunit electrodes (Plastics1, MS333/1-A/SPC) were placed onto the surface of the cortex in frontal (AP: +2 mm, ML: –3.5 mm) and parietal (AP: –6 mm, ML: –4 mm) areas for recording the electrical activity, along with the cerebellum for grounding (AP: –11 mm, ML: –2.5 mm). Electrodes were connected by insulated wires to a microconnector for the EEG recordings. Following the electrode placement, unjacketed optical fiber (250 µm core diameter, NA: 0.66; Prizmatix; glued with epoxy to a ferrule, 290 µm, NA: 0.66; Prizmatix) was engrafted into VB by a stereotaxic cannula holder, 0.2 mm dorsal to the virus injection site. Three stainless steel screws were then anchored to the skull, and optic fiber implants and electrodes were fixed with acrylic cement to stabilize the installation. The animal was removed from the stereotaxic apparatus and put in the vivarium room.

### In Vivo Electrophysiology

The EEG was continuously recorded via a four-channel electrophysiology system (Biopac MP36, CA, USA). The recording was performed with a sampling rate of 500 Hz and a 0.5 Hz to 100 Hz online bandpass filter. Each session started with a 1-h baseline recording (the first 30 min for habituation and the second 30 min for background EEG activity), followed by the optogenetic stimulation protocol. The poststimulation changes were recorded for half an hour.

## Optogenetic Stimulation

Optogenetic stimulations started after four weeks of virus injection to allow sufficient viral expression.<sup>37</sup> Optical fiber and ferrule were constructed using a do-it-yourself (DIY) kit (Prizmatix 2.5 mm/200  $\mu$ m). The light stimulation was controlled by a digital TTL pulser and delivered by an LED light source (Prizmatix, Dual LED, Holon, Israel) with a light intensity of 9.68 mW (Starter Kit 2). The rats were stimulated with 473-nm blue light in a plexiglass cage. The stimuli were delivered in 200 multiple square pulses (each pulse's duration was 50 ms) at 10 Hz<sup>36</sup> to the VB thalamus.

## Histology

After EEG recordings, all rats were injected with a high dose of ketamine (200 mg/kg) and xylazine (30 mg/kg) and transcardially perfused with phosphate-buffered saline and 4% paraformaldehyde. After careful removal from the skull, the brains were postfixed overnight in the same perfusion solution. The tissue was cryoprotected (0.1 M phosphate-buffered saline with 30% sucrose) the following day for at least two days at 4°C until use; 20- $\mu$ m coronal sections were cut using a cryostat (Leica CM 1950, Leica Biosys., Germany) for immunohistochemistry. The astrocyte-specific glial fibrillary acidic protein (GFAP) and neuronal nuclear protein (NeuN) staining procedures were performed to confirm the virus expression. Sections were washed four times in 0.1 M PBS for 5 min each and then incubated in a blocking solution comprising 1% BSA in 0.1% Triton-X/DPBS for 1 h at room temperature with gentle shaking. Sections were then incubated with primary antibodies diluted in “blocking solution” at 4°C. The following primary antibodies were used: anti-GFAP (1:100; Abcam Cat# ab7260) and anti-NeuN (1:100; Abcam Cat# ab177487) overnight at 4°C. The following day, sections were washed three times for 5 min with 0.1% Triton-X/DPBS and incubated for 1 h at room temperature with secondary antibody (Alexa 594; 1:100 for both). Finally, sections were washed, and nuclei were stained with 4', 6'-diamidino-2-phenylindole (DAPI; 0.5  $\mu$ g/mL in PBS) in an antifade mounting medium (Invitro, CA, USA) and then mounted on poly-lysine-coated glass. Stained sections were viewed using a confocal microscope (LEICA DMI8 SP8), and the images were analyzed using Las-X software. For immunostaining, based on the visual inspections, brain sections with needle tracks were chosen to study the glial activation after viral injection. Similarly, brain sections without needle tracks were selected for immunostaining to study the transgene's colocalization with other markers. The corresponding immunofluorescence imaging can be seen in Figure 1.

## Data Analysis

For each session, after a continuous 30-min baseline period, the effect of optogenetic stimulation was analyzed by the cumulative duration of SWD expressed as a percentage of the

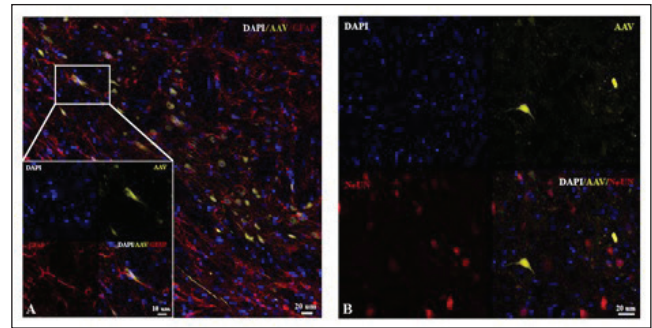


**Figure 1.** Selective expression of ChR2 in (A) astrocytes and (B) not in neurons.

total period of electrical activity recorded. Using Spike2 software (Cambridge Electronic Devices Ltd, Cambridge, UK), the peaks of each SWD were identified and expressed as instantaneous firing frequency. After extraction of spikes, their occurrence in terms of duration and total number were analyzed and compared between pre- (background) and post- (optogenetic) stimulation period.

For statistical analysis, the distribution of the data was tested using the Shapiro–Wilk test. Then, parametric paired *t*-test and nonparametric Mann–Whitney U test were used. The level of significance was selected as  $P < .05$ . All statistical analyses were performed using GraphPad Prism 8.3 (San Diego, USA).

## Results

### The Viral Reporters Were Specifically Expressed in VB Thalamus

To identify the GFAP-promoter-driven ChR2-expressing cells, we performed immunohistochemistry with GFAP antibody and high-magnification confocal imaging. The expression of the ChR2 virus was checked (Figure 1) and selective expression of GFAP was observed in astrocytes (Figure 1A), but not in neurons (Figure 1B).

### Optogenetic Stimulation of Astrocytes Increased the Cumulative Duration of SWDs in GAERS and the Number of SWDs in WAG-Rij

The optimized (50 ms, 200 times at 10 Hz) stimulation parameters were experimentally determined with the consideration of previous related works.<sup>37–39</sup> This illumination mode led to a change in seizure dynamic in increased epileptic activity in both GAERS and WAG-Rij rats. The cumulative line-length for cortical channels was used as a measure of the amplitude and frequency of each seizure to quantify the seizure dynamics.<sup>40</sup>

After the successful stereotaxic ChR2 injections in GAERS (Figure 2A), we observed the simultaneous SWD changes during optogenetic activation. The properties of the SWD and the cortical response to the VB thalamus



optogenetic stimulation were investigated in GAERS. The individual SWD was found to be long in duration and continuous (Figure 2B) regardless of the optogenetic stimulation. A representation of optogenetic stimulation pulses can be seen in Figure 2C. On the other hand, we found a significantly increased cumulative duration of the SWD period in Chr2-injected GAERS compared to their prestimulus background level ( $12.50 \pm 4.41$  s vs.  $17.44 \pm 6.07$  s (mean  $\pm$  SD);  $P = .0043$ ; Figure 2D). Furthermore, optogenetic stimulation did not produce any changes in the average SWD duration in control-virus-injected GAERS ( $18.62 \pm 4.94$  s vs.  $20.17 \pm 4.67$  s;  $P = .39$ ; Figure 2D). Moreover, the number of SWD bouts in Chr2-injected ( $28 \pm 12$  vs.  $24 \pm 9$ ;  $P = .13$ ) and control ( $21 \pm 9$  vs.  $22 \pm 8$ ;  $P = .92$ ) GAERS was not significantly affected by the stimulation compared to their background level (Figure 2E).

The effect of optogenetic stimulation of the VB thalamus on SWD characteristics was also investigated in WAG-Rij rats with correct injections (Figure 3A). The shapes of SWD in WAG-Rij were more variable within each burst than in GAERS (Figure 3B). A representation of optogenetic stimulation pulses can be seen in Figure 3C. Optogenetic stimulation did not change the duration of the SWD in both

control ( $3.81 \pm 1.37$  s vs.  $3.46 \pm 1.21$  s;  $P = .45$ ) and Chr2-injected ( $3.59 \pm 1.94$  s vs.  $3.47 \pm 2.07$  s;  $P = .62$ ) WAG-Rij (Figure 3D), in contrast to GAERS. However, VB thalamus stimulation significantly increased the number of SWD bouts in Chr2-injected WAG-Rij compared to background ( $18.52 \pm 11.46$  bursts/30 min vs.  $30.17 \pm 18.43$  bursts/30 min;  $P = .0015$ ; Figure 3E), but not in the control-virus-injected ones ( $16.17 \pm 10.77$  bursts/30 min vs.  $13.67 \pm 7.86$  bursts/30 min;  $P = .28$ ; Figure 3E).

### WAG-Rij had Higher Discharge Rate of SWD than GAERS

The firing rate of the spike components was calculated and examined (Figure 4). After detecting the instantaneous firing rate of randomly selected three bouts of SWD from each animal, we compared the firing rates of the SWD before and after the optogenetic stimulation. There was no difference in the firing rate of SWD in GAERS (background:  $6.77 \pm 0.42$  Hz vs. poststimulus:  $6.80 \pm 0.43$  Hz;  $P = .821$ ; Figure 4A) and in WAG-Rij rats (background:  $7.80 \pm 0.60$  Hz vs. poststimulus:  $7.90 \pm 0.72$  Hz;  $P = .66$ ; Figure 4B) before and after stimulation. However, both background ( $P < .0001$ ) and

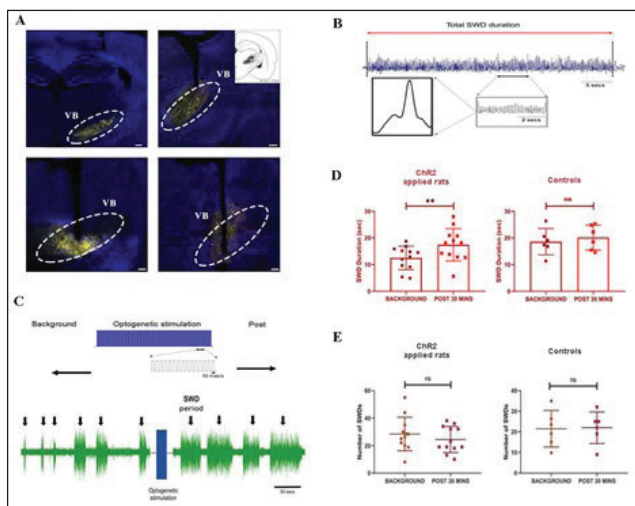


**Figure 2.** Injection and recording of GAERS animals. (A) Virus injection sites of the VB thalamus. (B) A sample recording of a burst of SWD. (C) Representation of the optogenetic stimulation pulses on the upper part. The lower part shows a sample figure depicting the electrophysiological recording. (D) The average duration of SWD before and after optogenetic stimulation in Chr2 (left) and control (right) virus injected GAERS. (E) The average number of SWD before and after optogenetic stimulation in Chr2 (left) and control (right) virus injected GAERS.  $**P < .01$ , Error bars are standard deviation. The background and poststimulus region were 30 min long. Scale bars of the images are 400  $\mu$ m for upper left, 200  $\mu$ m for upper right and below left, and 100  $\mu$ m for lower right.

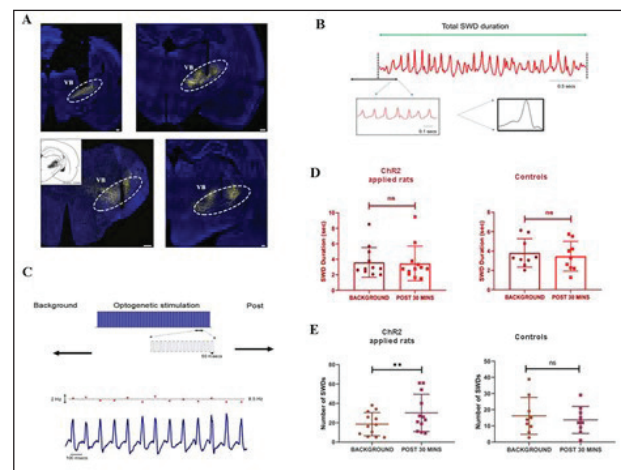


**Figure 3.** Injection and recording of WAG-Rij animals. (A) Virus injection sites of the VB thalamus. (B) A sample recording of a burst of SWD. (C) Representation of the optogenetic stimulation pulses on the upper part. The lower part shows a sample figure depicting the instantaneous firing rate of the SWD (red dots in the upper trace) and electrophysiological recording (lower trace). (D) The average duration of SWD before and after optogenetic stimulation in Chr2 (left) and control (right) virus injected WAG-Rij. (E) The average number of SWD before and after optogenetic stimulation in Chr2 (left) and control (right) virus injected WAG-Rij.  $**P < .01$ , Error bars are standard deviation. The background and poststimulus region were 30 min. Scale bars of the images are 300  $\mu$ m for upper left, 400  $\mu$ m for upper right and below left, and 200  $\mu$ m for the lower right.

poststimulus ( $P < .0001$ ) average firing rates of the SWD in WAG-Rij rats were significantly higher than the discharge rate recorded in GAERS (Figure 4C and D).

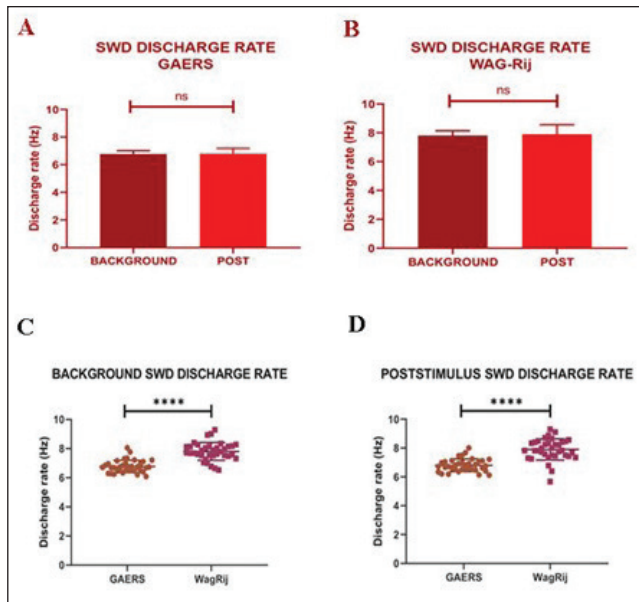


**Figure 4.** The difference between background and poststimulus SWD discharge rates in (A) GAERS and (B) WAG-Rij rats. The comparison of the (C) background and (D) poststimulus firing rates of SWD between GAERS and WAG-Rij. \*\*\*\* $P < .0001$ . Error bars are standard deviation.

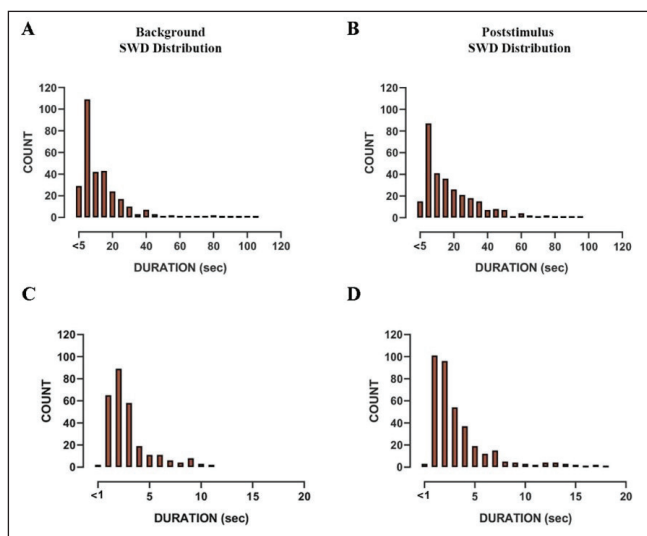


**Figure 5.** Histograms (5 s of bin width) showing the distribution of SWD duration at (A) background and (B) poststimulus region in GAERS. Histograms (1 s bin width) showing the distribution of SWD duration in WAG-Rij at (C) background and (D) poststimulus region.

### SWD Duration Distribution Was Similar in Both Rat Models Before and After Optogenetic Stimulation

In Chr2-injected GAERS, the majority of the SWD durations in background and poststimulus were ranged from 5 to 20 s. There were occasional long SWDs recorded at both background and poststimulus that lasted over a minute (Figure 5A and B). The SWD in Chr2-injected WAG-Rij had also a similar duration in the background and poststimulus phases. The majority of SWD ranged between 1 s and 3 s in the background, whereas it was between 1 s and 4 s in the poststimulus phases (Figure 5C and D).

### Discussion

In this study, the optogenetic excitation of the astrocytes of the VB thalamus showed a significant increase in the duration of SWD in GAERS. The SWD in WAG-Rij did not have significant changes in duration but did show an increase in the number of SWD. These results show that the optogenetically activated astrocytes in the VB thalamus affect the SWD activity of cortical neurons in the AE with different outcomes in the two mostly used animal models of this disease.

Recent studies suggest that in the pathogenesis of AE, glial cells can change homeostatic network functions that temporally precede alterations in neurons and thus seem to be causative for this disorder.<sup>41–43</sup> An increase in the expression of GFAP in the cortex and thalamus of GAERS was reported,<sup>44</sup> which in turn may modify astrocytic functions<sup>45</sup> and interfere with the process giving rise to seizures.<sup>44</sup> In accordance with the above-mentioned findings, our previous study demonstrated a significant increase in GFAP-positive astrocyte populations and GFAP protein expression in the VB thalamus of GAERS and WAG-Rij compared to control rats.<sup>46</sup>

There is mounting evidence suggesting that astrocytes modulate neuronal excitability through the release of gliotransmitters. Calcium-dependent glutamate release from astrocytes has attracted particular attention in the context of epilepsy.<sup>27,47,48</sup>  $Ca^{2+}$ -dependent glutamate release may exaggerate epileptic activity by an excitatory feedback loop or even trigger epileptic activity through NMDA receptors.<sup>23,30–32</sup> Whether the epileptiform activity is a direct cause of astrocytic glutamate release is still unclear,<sup>23,30</sup> and the exact signaling mechanism remains to be determined. In the developing thalamus, astrocytes display spontaneous calcium oscillations that are not dependent on previous neuronal activity and are correlated with NMDA-receptor-mediated currents recorded in neighboring neurons.<sup>9</sup> The stimulation of astrocytic calcium increases also leads to inward currents in neighboring neurons,<sup>9</sup> indicating that activity arising in astrocytes can induce activity in neurons.

Astrocytes also showed coordinated increases in  $\text{Ca}^{2+}$ , and calcium waves were seen to propagate between astrocytes in the VB thalamus.<sup>13</sup>

Previously, cell culture studies on the propagation of astrocytic calcium waves showed that the transmission occurs via gap junctions<sup>49,50</sup> or chemically with ATP and glutamate.<sup>50,51</sup> Parpura et al.<sup>52</sup> used flash photolysis in astrocyte–neuron cocultures to increase astrocytic calcium levels and revealed that raising astrocytic calcium within physiological levels leads to the release of glutamate and concurrent neuronal inward currents. In our current study, the optogenetic manipulation of thalamic astrocytes changed the cortical neuronal response seen in SWD in GAERS and WAG-Rij. Regarding GAERS, optogenetic stimulation caused a significant increase in the cumulative duration of SWDs in the 30-min poststimulation period. In WAG-Rij, it was shown that the number of SWD in the poststimulation period was significantly increased. These results indicate that astrocytes can cause different SWD expressions in GAERS and WAG-Rij.

The exact mechanisms of the astrocyte–neuron interaction remain unidentified; however, studies are showing the possible candidates.<sup>27,28,53,54</sup> The existence of the vesicle-associated SNARE protein synaptobrevin in astrocytes was earlier described,<sup>55</sup> and Araque et al.<sup>53</sup> showed that the selective cleavage of synaptobrevin by botulinum B neurotoxin was able to block the astrocytic–glutamate-induced inward currents in neurons. The study reveals that calcium-dependent glutamate release from astrocytes is a SNARE protein-dependent event and suggests that glutamate in astrocytes is stored in vesicles and released via the exocytotic pathway. Further studies should be performed on the exact mechanisms of astrocyte–neuron interactions in terms of possible mechanistic explanations, as exemplified above.

The increasing number of studies showed that the manipulation of astrocytes via optogenetic is a novel method to activate astrocytes.<sup>7,8,37,39,56</sup> Modulatory effects of astrocytes in response to optogenetic activation were shown by Perea et al.<sup>39</sup> They showed that astrocytes regulate the response selectivity of the visual cortex neurons. Moreover, light stimulation of ChR2-expressing astrocytes in the visual cortex increased the frequency of spontaneous excitatory and inhibitory postsynaptic currents in adjacent neurons in an mGluR1-dependent manner, suggesting that glutamate is the responsible gliotransmitter in response to optogenetic stimulation. Also, neuronal membrane potentials did not show shifts synchronized with astrocyte photostimulation, indicating no direct action of photostimulation of astrocytes on neurons.

Furthermore, glutamate release from astrocytes after ChR2 stimulation was directly shown in cerebellar astrocytes.<sup>8</sup> Optogenetic activation of cerebellar astrocytes results in AMPA receptor activation on Purkinje cells and enhanced long-term depression of the synapses between parallel fibers

to Purkinje cells. These studies demonstrate that astrocyte ChR2 stimulation successfully regulates astrocyte activity and supports that astrocyte gliotransmitter release and subsequent synaptic transmission can be regulated by optogenetic stimulation, which can be a useful approach to uncover the patho/physiological role of astrocytes in brain functions. Our study showed that optogenetic stimulation of astrocytes affected the SWD kinetics, albeit in different patterns in GAERS and WAG-Rij. Although mostly descriptive, the results point to interesting differences in the two SWD models and suggest that SWDs in these two rat models are likely driven by similar yet distinct mechanisms. It remains to be clarified fully how the optogenetic stimulation enhances physiological changes in astrocytes and, subsequently, neurons and what are the cellular and/or molecular mechanisms underlying the different responses of GAERS and WAG-Rij.

Overall, although the exact mechanistic explanation of how optogenetic manipulation of astrocytes affects the synaptic transmission remains to be identified, literature so far suggests that the main candidate is the increased  $\text{Ca}^{2+}$  levels in astrocytes after optogenetic manipulation<sup>7,9,39</sup> and subsequent gliotransmitter release<sup>8</sup> with various intracellular communications.<sup>50,51,53</sup>

Although both inbred GAERS and WAG-Rij rats are well-validated genetic models of AE, structural and anatomical differences, including the increased amygdala and ventricular volumes, thickness in the somatosensory cortex, and callosal and fornical abnormalities, between the two strains exist.<sup>57–59</sup> An enhanced cortical excitation<sup>60</sup> and alterations in GABAergic synaptic transmission properties in various thalamic nuclei neurons were reported in GAERS.<sup>61</sup> However, cortical excitability of the somatomotor cortex was not validated in WAG-Rij rats.<sup>62</sup> Environmental conditions and genetic drift have a different impact on the severity of epilepsy between the two strains.<sup>63</sup> Our study revealed that although there was no difference in the firing rate of each SWD before and after the optogenetic stimulation in GAERS or WAG-Rij, the average firing rate of the SWD in WAG-Rij rats was significantly higher than in GAERS. Akman et al.<sup>64</sup> compared the EEG phenotype of GAERS and WAG-Rij rats and showed that GAERS present a significantly higher number, cumulative duration, and mean duration of SWD than WAG-Rij. At the same time, the cycle frequency of the discharges of SWD was higher in the WAG-Rij rats. Our study shows that GAERS display 5 s to 20 s SWD whereas WAG-Rij rats display 1 s to 4 s SWD following optogenetic stimulation of the VB thalamus, which is in line with the aforementioned study. The results of the present and former studies comparing the two strains showed differences in frequency and amplitude of SWD, with distinct pharmacological,<sup>65</sup> genetic,<sup>66</sup> and ontogenetic profiles.<sup>67</sup> Therefore, these models are phenotypically and genetically distinct.



## Technical Remarks

The astrocyte-specific virus used in the present study was expressed in thalamic astrocytes.<sup>37,68–70</sup> Tian et al.<sup>23</sup> showed that stimulation of neurons using the same method as astrocytes showed no field potential generation, whereas the astrocyte stimulation triggers calcium-dependent glutamate release, resulting in paroxysmal discharge shifts in neighboring neurons. Further studies are required to fully understand the molecular mechanisms underlying the ChR2-induced changes in astrocytes and their effects on various brain functions.

## Limitations of the Study

The preliminary preparation is highly important for the success of the optogenetic experimentation. The optimal injection site, concentration, and expression time for opsin and the optimization of the light intensity and duration are critical. In order to prevent nonspecific effects of opsin expression and light delivery, these parameters should be carefully evaluated.

The main advantage of optogenetics is that channels can target specific cell types and manipulate the activity of individual cells under the control of specific promoters. The subtypes of astrocytes could play different roles in the neural network. However, the specific promoters for the subtypes of astrocytes are not present. In addition, how optogenetic manipulation affects the SWD also needs to be explored at the molecular level. Therefore, further studies are necessary regarding the molecular changes in the neurotransmitter turnover and transmission in AE.

## Conclusion

The results of the present study show that the astrocytes contribute to the different aspects of the pathophysiology of AE. The study also provides information about the differences in two different animal strains. ChR2-derived light-sensitive effectors on studying astrocytes illustrate their potential usage in the understanding of astrocyte-to-neuron interaction while the current available optogenetic actuators successfully initiate biologically relevant signaling events in astrocytes.<sup>71</sup> Altogether, the present study may pave the way for the development of astrocyte-related therapeutic interventions for the pharmacological treatment of absence seizures.

## Acknowledgments

The authors would like to thank the Koç University Research Center for Translational Medicine (KUTTAM) for using the facilities. The authors would also like to thank Prof. Kemal Türker for his support in the availability of the electrophysiological equipment and Professor Filiz Onat for providing the GAERS animals.

## Authors' Contribution

All authors contributed to the study conception. MÖ, MGÖ and SC were responsible for conceiving and designing the study. Optogenetic set up was designed by MÖ, MGÖ and SA. The material preparation and data collection were performed by MÖ. Data analysis were performed by MGÖ and MÖ. The project was guided by SC. The first draft of the manuscript was written by MÖ; all authors commented on previous versions of the manuscript. All authors read and approved the final manuscript.

## Statement of Ethics

All experimental conditions and procedures were performed in compliance with the National Institutes of Health (NIH) regulations of animal care covered in the Guide for the Care and Use of Laboratory Animals (2011). The local Animal Ethics Committee of Koç University approved all the procedures. The study was conducted at the Koç University Research Center for Translational Medicine (KUTTAM). The study was approved by the Local Animal Ethics Committee of Koç University under approval number 2018.HADYEK.017.

## Declaration of Conflicting Interests

The authors declared no potential conflicts of interest with respect to the research, authorship, and/or publication of this article.

## Funding

The authors received no financial support for the research, authorship, and/or publication of this article.

## ORCID iD

Merve Ozgur  <https://orcid.org/0000-0002-0909-8433>

## References

1. Vasile F, Dossi E, and Rouach N. Human astrocytes: Structure and functions in the healthy brain. *Brain Struct Funct* 2017; 222(55): 2017–2029.
2. Eroglu C and Barres BA. Regulation of synaptic connectivity by glia. *Nature* 2010; 468: 223–231.
3. Perea G, Navarrete M, and synapse: Araque A. Tripartite Astrocytes process and control synaptic information. *Trend Neurosci* 2009; 32: 421–431.
4. Araque A, Parpura V, Sanzgiri RP, et al. Glutamate-dependent astrocyte modulation of synaptic transmission between cultured hippocampal neurons. *Eur J Neurosci* 1998; 10: 2129–2142.
5. Araque A, Sanzgiri RP, Parpura V, et al. Astrocyte-induced modulation of synaptic transmission. *J Physiol Pharmacol* 1999; 77: 699–706.

6. Newman EA and Zahs KR. Calcium waves in retinal glial cells. *Science* 1997; 275: 844–847.
7. Gourine AV, Kasymov V, Marina N, et al. Astrocytes control breathing through pH-dependent release of ATP. *Science* 2010; 329: 571–575.
8. Sasaki T, Beppu K, Tanaka KF, et al. Application of an optogenetic byway for perturbing neuronal activity via glial photostimulation. *Proc Natl Acad Sci USA* 2012; 109: 20720–20725.
9. Parri HR, Gould TM, and Crunelli V. Spontaneous astrocytic Ca<sup>2+</sup> oscillations in situ drive NMDAR-mediated neuronal excitation. *Nat Neurosci* 2001; 4: 803–812.
10. Kidd FL, Isaac JT, and Isaac TR. Kinetics and activation of postsynaptic kainite receptors at thalamocortical synapses: Role of glutamate clearance. *J Neurophysiol* 2001; 86: 1139–1148.
11. Schummers J, Yu H, and Sur M. Tuned responses of astrocytes and their influence on hemodynamics signals in the visual cortex. *Science* 2008; 320: 1638–1643.
12. Wang X, Lou N, Xu Q, et al. Astrocytic Ca<sup>2+</sup> signaling evoked by sensory stimulation in vivo. *Nat Neurosci* 2006; 9: 816–823.
13. Parri HR, Gould TM, and Crunelli V. Sensory and cortical activation of distinct glial cell subtypes in the somatosensory thalamus of young rats. *Eur J Neurosci* 2010; 32: 29–40.
14. Tenney RJ and Glauser TY. The current state of absence epilepsy: Can we have your attention? *Epilep Curr* 2013; 13: 135–140.
15. Meeren HKM, Pijn JPM, Van Luijckelaar LJM, et al. Cortical focus drives widespread corticothalamic networks during spontaneous absence seizures in rats. *J Neurosci* 2002; 22: 1480–1495.
16. Blumenfeld H and McCormick DA. Corticothalamic inputs control the pattern of activity generated in thalamocortical networks. *J Neurosci* 2000; 20: 5153–5162.
17. Gloor P. Generalized cortico-reticular. Some considerations on the pathophysiology of generalized bilaterally synchronous spike and wave discharge. *Epilepsia* 1968; 9: 249–263.
18. De Curtis M and Avanzini G. Thalamic regulation of epileptic spike and wave discharges. *Funct Neurol* 1994; 9: 307–326.
19. Blumenfeld H. The thalamus and seizures. *Arch Neurol* 2002; 59: 135–137.
20. Vergnes M and Marescaux C. Cortical and thalamic lesions in rats with genetic absence epilepsy. *J Neural Transm Suppl* 1992; 35: 71–83.
21. Avanzini G, de Curtis M, Marescaux C, et al. Role of the thalamic reticular nucleus in the generation of rhythmic thalamocortical activities subserving spike and waves. *J Neural Transm Suppl* 1992; 35: 85–95.
22. Meeren HKM, Veening JG, Modersheim TAE, et al. Thalamic lesions in a genetic rat model of absence epilepsy: Dissociation between spike-wave discharges and sleep spindles. *Exp Neurol* 2009; 217: 25–37.
23. Tian GF, Azmi H, Takano T, et al. An astrocytic basis of epilepsy. *Nat Med* 2005; 11: 973–981.
24. Yamamura S, Hoshikawa M, Dai K, et al. ONO-2506 inhibits spike-wave discharges in a genetic animal model without affecting traditional convulsive tests via gliotransmission regulation. *Br J Pharmacol* 2013; 168: 1088–1100.
25. Uhlmann EJ, Wong M, Baldwin RL, et al. Astrocyte-specific TSC1 conditional knockout mice exhibit abnormal neuronal organization and seizures. *Ann Neurol* 2002; 52: 285–296.
26. Tanaka K, Watase K, Manabe T, et al. Epilepsy and exacerbation of brain injury in mice lacking the glutamate transporter GLT-1. *Science* 1997; 276: 1699–1702.
27. Parpura V, Basarsky TA, Liu F, et al. Glutamate-mediated astrocyte-neuron signaling. *Nature* 1994; 369: 744–747.
28. Pasti L, Voltera A, Pozzan T, et al. Intracellular calcium oscillations in astrocytes: A highly plastic, bidirectional form of communication between neurons and astrocytes in situ. *J Neurosci* 1997; 17: 7817–7830.
29. Henneberger C. Does rapid and physiological astrocyte-neuron signaling amplify epileptic activity? *J Physiol* 2017; 595: 1917–1927.
30. Fellin T, Sul JY, D’Ascenzo M, et al. Bidirectional astrocyte-neuron communication: The many roles of glutamate and ATP. *Novartis Found Symp* 2006; 276: 208–217.
31. Gomez-Gonzalo M, Losi G, Chiavegato A, et al. An excitatory loop with astrocytes contributes to drive neurons to seizure threshold. *Plos Biol* 2010; 8: e1000352.
32. Crunelli V and Carmignoto G. New vistas on astroglia in convulsive and nonconvulsive epilepsy highlight novel astrocytic targets for treatment. *J Physiol* 2013; 591: 775–785.
33. Danober L, Deransart C, Depaulis A, et al. Pathophysiological mechanisms of genetic absence epilepsy in the rat. *Prog Neurobiol* 1998; 55: 27–57.
34. Depaulis A and Van Luijckelaar G. Genetic models of absence epilepsy in the rat. In: Pitkanen A, Schwartzkroin PA, Moshe S (eds). *Models of Seizures and Epilepsy*. Elsevier Academic, 2006, 2006, 233–247.
35. Lazic SE. Four ways to increase power without increasing the sample size. *Lab Anim* 2018; 52(6): 621–629.
36. Paxinos G and Watson C. *The Rat Brain in Stereotaxic Coordinates*. 5th ed. Academic press; 2004: 30–34.
37. Pelluru D, Konadhode RR, Bhat NR, et al. Optogenetic stimulation of astrocytes in the posterior hypothalamus increases sleep at night in C57BL/BJ mice. *Eur J Neurosci* 2016; 43: 1298–1306.
38. Yizhar O, Fenno LE, Davidson TJ, et al. Optogenetics in neural systems. *Neuron* 2011; 14: 9–34.
39. Perea G, Yang A, Es Boyden, et al. Optogenetic astrocyte activation modulates response selectivity of visual cortex neurons in vivo. *Nat Commun* 2014; 5: 3262.
40. Guo L, Rivero D, Dorado J, et al. Automatic epileptic seizure detection in EEGs based on length feature and artificial neural networks. *J Neurosci Methods* 2010; 191: 101–109.
41. Cavdar S, Bay HH, Ö Kirazli, et al. Comparing GABAergic cell populations in the thalamic reticular nucleus of normal and genetic absence epilepsy rats from Strasbourg (GAERS). *Neurol Sci* 2013; 34: 1991–2000.
42. Danbolt NC. Glutamate uptake. *Prog Neurobiol* 2001; 65: 1–105.
43. Pirttimäki T, Parri HR, and Crunelli V. Astrocytic GABA transporter GAT-1 dysfunction in experimental absence seizures. *J Physiol* 2013; 591: 823–833.
44. Dutuit M, Didier-Bazes M, Vergnes M, et al. Specific alteration in the expression of glial fibrillary acidic protein, glutamate dehydrogenase, and glutamine synthetase in rats with genetic absence epilepsy. *GLIA* 2000; 32: 15–24.
45. Ridet JL, Malhotra SK, Privat A, et al. Reactive astrocytes: Cellular and molecular cues to biological function. *Trends Neurosci* 1997; 20: 570–577.
46. Cavdar S, Kuvvet Y, Sur-Erdem I, et al. Relationships between astrocytes and absence epilepsy. *Neurosci Lett* 2019; 712: 134518.
47. Shigetomi E, Tong X, Kwan KY, et al. TRPA1 channels regulate astrocyte resting calcium and inhibitory synapse efficacy through GAT-3. *Nat Neurosci* 2012; 15: 70–80.



48. Li D, Herault K, Isacoff EY, et al. Optogenetic activation of LiGluR-expressing astrocytes evokes anion channel-mediated glutamate release. *J. Physiol* 2009; 590: 855–873.
49. Giaume C and Venance L. *Intercellular calcium signaling and gap junctional communication in astrocytes*. *Glia* 1998; 24: 50–64.
50. Newman EA. Propagation of intercellular calcium waves in retinal astrocytes and Muller cells. *J Neurosci* 2001; 21: 2215–2223.
51. Cotrina ML, Lin JH, and Nedergaard. Cytoskeletal assembly and ATP release regulate astrocytic calcium signaling. *J Neurosci* 1998; 18: 8794–8804.
52. Parpura V, Basarsky TA, Liu F, et al. Physiological astrocytic calcium levels stimulate glutamate release to modulate adjacent neurons. *Proc Natl Acad Sci USA* 2000; 97: 8629–8634.
53. Araque A, Li N, Doyle RT, et al. Snare protein dependent glutamate release from astrocytes. *J Neurosci* 2000; 20: 666–673.
54. Pasti L, Zonta M, Pozzan T, et al. Cytosolic calcium oscillations in astrocytes may regulate exocytotic release of glutamate. *J Neurosci* 2001; 21: 477–484.
55. Parpura V, Fang Y, Basarsky T, et al. Expression of synaptobrevin II, cellubrevin and syntaxin but not SNAP-25 in cultured astrocytes. *FEBS Lett* 1995; 377(3): 489–492.
56. Yamashita A, Hamada A, Suhara Y, et al. Astrocytic activation in the anterior cingulate cortex is critical for sleep disorder under neuropathic pain. *Synapse* 2014; 68: 235–247.
57. Powel KL, Tang H, Ng C, et al. Seizure expression, behavior, and brain morphology differences in colonies of genetic absence epilepsy rats from Strasbourg. *Epilepsia* 2014; 55: 1959–1968.
58. Clasadonte J, Dong J, Hines DJ, et al. Astrocyte control of synaptic NMDA receptors contribute to the progressive development of temporal lobe epilepsy. *Proc Natl Acad Sci USA* 2013; 110: 17540–17545.
59. Karpova AV, Bikbaev AF, Coenen A, et al. Morphometric Golgi study of cortical locations in WAG-Rij rats: The cortical focus theory. *Neurosci Res* 2005; 51: 119–128.
60. Richards DA, Lemos T, Whitton PS, et al. Extracellular GABA in the ventrobasal thalamus of rats exhibiting spontaneous absence epilepsy: A microdialysis study. *J Neurochem* 1995; 65: 1674–1680.
61. Bessaih T, Bourgeois L, Badiu CI, et al. Nucleus-specific abnormalities of GABAergic synaptic transmission in a genetic model of absence seizures. *J Neurophysiol* 2006; 96: 3074–3081.
62. Tolmacheva EA, Van Luijtelaar G, Chepurinov SA, et al. Cortical and limbic excitability in rats with absence epilepsy. *Epilepsy Res* 2004; 62: 189–198.
63. Schridde U and Van Luijtelaar G. The role of the environment on the development of pike-wave discharged in two strains of rats. *Physiol Behav* 2005; 84: 379–386.
64. Akman O, Demiralp T, Ates N, et al. Electroencephalogram differences between WAG-Rij and GAERS rat models of absence epilepsy. *Epilepsy Res* 2010; 89: 185–193.
65. Midzianovskaia IS, Kuznetsova GD, Coenen AM, et al. Electrophysiological and pharmacological characteristics of two types of spike-wave discharges in WAG-Rij rats. *Brain Res* 2001; 911: 62–70.
66. Gauguier D, Bihoreau MT, Wilder SP, et al. Chromosomal mapping of genetic loci controlling absence epilepsy phenotypes in the WAG-Rij rat. *Epilepsia* 2004; 45: 908–915.
67. Rudolf G, Bihoreau TM, Godfrey RF, et al. Polygenic control of idiopathic generalized epilepsy phenotypes in the genetic absence rats from Strasbourg (GAERS). *Epilepsia* 2004; 45: 301–308.
68. Lawlor PA, Bland RJ, Mouravlev A, et al. Efficient gene delivery and selective transduction of glial cells in the mammalian brain by AAV serotypes isolated from nonhuman primates. *Mol Ther* 2009; 17: 1692–1702.
69. Poskanzer KE and Yusre R. Astrocytes regulate cortical state switching in vivo. *PNAS* 2016; 113: e2675–e2684.
70. Adamsky A, Kol A, Kreisel T, et al. Astrocytic activation generates de novo neuronal potentiation and memory enhancement. *Cell* 2018; 174: 59–71.
71. Figueiredo M, Lane S, Stout RF, et al. Comparative analysis of optogenetic actuators in cultured astrocytes. *Cell Calcium* 2014; 56: 208–214.